Surface characteristics of silver oxide thin film electrodes for supercapacitor applications

Mirzaeian, Mojtaba; Ogwu, Abraham A.; Jirandehi, Hassan Fathinejad; Aidarova, Saule; Ospanova, Zhanar; Tsendzughul, Nathaniel

Published in:
Colloids and Surfaces A: Physicochemical and Engineering Aspects

DOI:
10.1016/j.colsurfa.2016.04.026

Published: 20/04/2017

Surface Characteristics of Silver Oxide Thin Film Electrodes for Supercapacitor Applications

Mojtaba Mirzaeian [a,*], Abraham A Ogwu [a], Hassan Fathinejad Jirandehi [b], Saule Aidarova [c], Zhanar Ospanova [d], Nathaniel Tsendzughul [a]

[a] *School of Engineering and Computing, University of the West of Scotland, Paisley, PA1 2BE, Scotland, UK.*
[b] *Department of Chemistry, Islamic Azad University, Farahan Branch, Farahan, Arak, Iran.*
[c] *Kazakh National Research Technical University named after K.I.Satpayev, International Postgraduate Institute "Excellence PolyTech", Almaty, Kazakhstan*
[d] *Faculty of Chemistry and Chemical Technology, Al-Farabi Kazakh National University, Almaty, Kazakhstan*

Abstract

In this paper the preparation of nano-structured silver oxide thin films with different oxidation states with promise as electrode materials for supercapacitors by reactive magnetron sputtering is investigated. The chemical, structural, surface morphological dependence of the films on oxygen gas flow rate and deposition power were examined by scanning electron microscope (SEM), X-ray diffraction (XRD) and energy dispersive X-ray (EDX). The average thickness of the films was controlled in the range of ≈ 50 – 330 nm. The XRD spectra of the films indicated the formation of bi-phase films comprised of silver and silver oxides with different oxidation states. The wettability of the films in contact with different probing liquids was investigated by measuring the contact angles using a goniometer. It was shown that the silver oxide films are relatively hydrophilic and increasing oxygen flow rate increases the wettability of the films toward water as a result of increase in the oxidation state of the films and consequently clustering of electrons in polar molecules of water around the oxides at higher oxidation states. This is further confirmed by the analysis of the surface energy measurements.

Keywords: Thin film electrode; Silver oxide; Oxidation state; Wettability; Surface energy; Reactive magnetron sputtering

*Corresponding author: E-mail address: mojtaba.mirzaeian@uws.ac.uk (M. Mirzaeian), Fax: +44 141 848 3404

1. INTRODUCTION

Among different energy storage technologies, electrochemical capacitors have, especially, shown great potential in recent years to meet the short-term power needs and energy demands. They are mainly classified into two broad categories known as electrical double-layer capacitors and pseudocapacitors, based on their charge-storage mechanism. Pseudocapacitors store electrical energy through reversible faradaic redox reactions in which the oxidation state of the electro-active material utilized in electrodes changes during electron transfer. In theory, their capacitive ability is expected to be much higher than that of the double-layer capacitors in which the capacitance arises from electrostatic charge separation at the interface between a conductive electrode and an adjacent liquid electrolyte.

Many metal oxides exhibit pseudocapacitive behavior over small ranges of potential that results in Faradaic charge transfer across the double-layer leading to electrochemical processes involving Faradaic and non-Faradaic energy storage simultaneously, with a degree of electron transfer in the range of 1–2.5 e^- per atom of accessible surface of electroactive material. These materials show much higher capacitance compared with the capacitive capability of double-layer capacitors where a much lower degree of electron transfer (between 0.17–0.2 e^- per atom of accessible surface) happens [1].

Chemical and structural reversibility of reactions occurring in the charge/discharge process, high electrical conductivity, high surface area, and both electron and proton hopping in the oxide lattice are the main inevitabilities for the employment of metal oxides as electro-active material for pseudocapacitor applications. Ruthenium dioxide, RuO_2, exhibits a metallic electronic conductivity and significant pseudocapacitive behavior, with the highest reported specific capacitance (ca. 850 F g^{-1}) which is fairly constant over a relatively wide potential range making it as a superior material for supercapacitor applications. However the use of RuO_2 has mainly been limited to small-scale devices since it is prohibitively expensive for large scale applications [2]. In search for less expensive alternatives to RuO_2, other metal oxides such as manganese oxides, nickel oxides, cobalt oxides, vanadium oxides and iron oxides have been explored over the past decade [3-7]. Although these compounds have shown promise as electrode materials and various synthesis methods have been used to produce them with different morphologies and pore characteristics, as yet, commercialization of metal oxide based supercapacitors has been mired, since the electrical conductivity of the alternative metal oxides is drastically lower than that of RuO_2.

As the purpose of a supercapacitor is to store energy and release it quickly in a controlled manner with a high power capability and very high degree of reversibility (lifetimes in excess of 10^6

cycles), the utilization of a highly conductive pseudocapacitive metal oxide as electrode material with optimized structural and surface properties that enables fast redox reactions through shortened diffusion path in solid phase is vital. Therefore the main objective of this work is to investigate the morphological, chemical and wettability properties of silver oxide thin films with different oxidation states prepared by reactive magnetron sputtering as potential electrode materials for supercapacitor applications. As silver in oxidation state (AgO, Ag_2O, Ag_2O_2) is more conductive than other transition metal oxides investigated for electrochemical capacitor (EC) applications, it would be expected to act as a superior candidate for electrode material in electrochemical capacitors. This new thinking about the employment of nano-structured silver oxide thin film electrodes will have a definite impact on research into the development of high voltage electrochemical supercapacitors and optimizing their energy storage and power capability. Such an investigation is therefore timely not only because of the current interest in high performance supercapacitors, but also from the scientific point of view.

1.1. Theory of contact angle and surface energy measurements

When a liquid is in contact with a solid there is a force of attraction between molecules of a liquid balanced in all directions within the liquid itself, except at its interface with the solid surface where attractive and repulsive forces exist between molecules of liquid and the solid surface in contact with them. The net effect of this imbalanced force creates the presence of free energy at the surface of a liquid. This net energy is the surface free energy [8].

Contact angle is the angle formed by a liquid at the three phase boundary where a liquid, solid and gas intersect. Figure 1 shows a schematic diagram of the contact angle at solid-liquid-vapor interface.

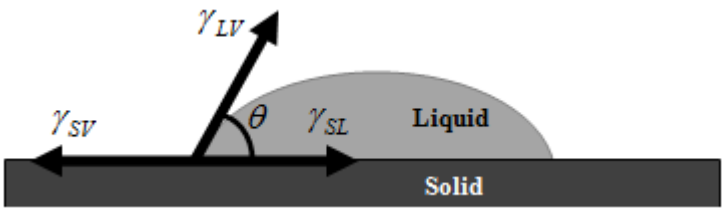

Figure 1: Contact angle at solid-liquid-vapor interface

The contact angle measures the level of wettability of a solid by a liquid. The contact angle that a liquid drop makes with a solid surface serves as a dual purpose- evaluation of surface energy as well as determination of hydrophilicity and hydrophobicity of the surface [9].

The equation governing the behavior of a liquid drop on a surface and relating contact angle measurement and key thermodynamic parameters of a surface is given by Thomas Young as [9, 10]:

$$\gamma_{SV} = \gamma_{SL} + \gamma_{LV} \, Cos\theta \qquad (1)$$

Where γ_{SV}, γ_{LV} and γ_{SL} are the surface energy of the solid, the free energy of the liquid and the surface energy of the solid-liquid interface considered as the thermodynamic interfacial energy parameters for solid-vapor, liquid- vapor and solid –liquid respectively and θ is the contact angle.

According to Fowkes, Owens and Wendt; surface energy can be split into dispersive component γ^d due to Van der Walls and London forces and a polar component γ^p due to hydrogen bonds and dipole-dipole interactions[11, 12]. The total surface energy is therefore the sum of these two components [13].

$$\gamma^{Tot} = \gamma^p + \gamma^d \qquad (2)$$

Where γ^d, γ^p and γ^{Tot} are the polar, dispersive and total surface energies respectively.

In acid based approach also known as Van Oss-Chaudhury- Good method, the total surface free energy of a solid is composed of two parts: the Lifshitz-van der Waals dispersive component γ_s^{LW} and the acid-base polar component γ_s^{AB} [12].

$$\gamma^{Tot} = \gamma_s^{LW} + \gamma_s^{AB} \qquad (3)$$

The Lifshitz-van der Waals component is the nonpolar electrodynamic component which includes the long-range interactions contributed by London, Debye and Keesom pole interactions while the acid-base component contains the short-range acid-base interactions contributed by hydrogen bonding having a non-additive electron acceptor (γ^+) and electron donor (γ^-). The term γ^{AB} is equal to double mean geometrical value of acid (γ^+) and base (γ^-) interactions as follow [13, 14]

$$\gamma_s^{AB} = 2\left(\gamma^+ \gamma^-\right)^{1/2} \qquad (4)$$

Contact angle and surface energy measurements provide information on the wettability of surfaces and determine whether a liquid droplet sticks /or is removed from a surface or it spreads or remain at the point of contact.

2. EXPERIMENTAL

2.1. Film Deposition

The deposition of thin films on glass substrates were carried out in a cryo-pumped vacuum chamber (CVC) magnetron sputtering unit using pure solid silver target as the starting material with high purity argon and oxygen as sputtering and reactive gases, respectively. Depositions were performed at different oxygen flow rates ranging between 0 to 10 standard cubic centimeters per minute (sccm) and different forward deposition powers in the range of 100 to 400W. Prior to the deposition, the substrates were cleaned ultrasonically in iso-propanol and then washed with de-ionized water and the deposition chamber was evacuated to the pressure of about 8µTorr. All samples were deposited at a base pressure of 2.5mTorr. Depositions were performed at deposition times of 2 and 5 minutes with a reflective power less than 5% of the forward power during the deposition.

2.2. Contact angle measurements

Contact angle and surface energy measurements were performed with a fully computer controlled goniometer system (KSV CAM 200) based on video capture of images and automatic image analysis using CAM software. Static contact angles and surface free energies were measured using water, ethylene glycol and diiodomethane as the probing liquids with accuracy of ± 0.1 degree and ± 0.01 mJ/m^2 respectively.

3. RESULTS AND DISCUSSION

3.1. SEM and EDX results

The silver and silver oxides thin films were deposited on the glass substrate at zero and higher oxygen flow rates in the range of 2 to 10sccm respectively. The surface morphology of the deposited thin films was investigated by scanning electron microscope (SEM).

Figure 2 shows typical SEM micrographs (cross sectional view) of varying thicknesses of the thin films for varying deposition powers and O_2 flow rates. Digital images of deposited thin films obtained by SEM show that the average thickness of the films can be controlled in the range of 50 – 330 nm when varying the oxygen flow rate and the deposition forward power. The thickness of the silver oxide films increases with increase in the deposition power. A decrease in the film thickness with increasing the O_2 flow rate was noticed. This might be due to the formation of thin film of

silver oxide with different oxidation states at higher oxygen flow rates. It was noticed that here is a three-fold increase in the film thickness as the deposition time is increased from 2 to 5 min.

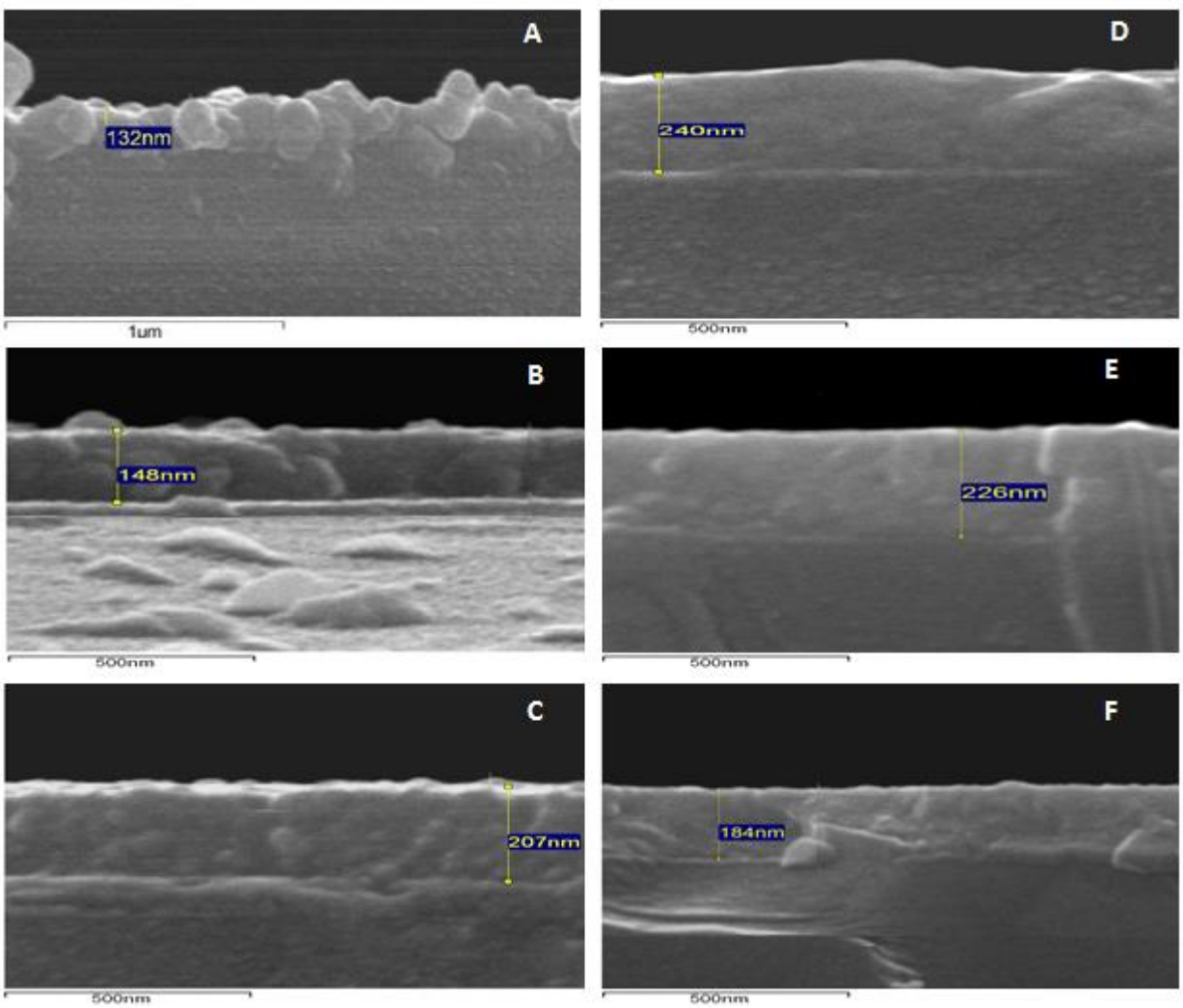

Figure 2: SEM micrographs of the thicknesses of thin films at different power and O_2 flow rates with deposition time of 2 minutes. A(100W, 4sccm O_2), B(200W, 4sccm O_2), C(250W, 4sccm O_2), D(300W O_2, 4sccm O_2), E(300W, 8sccm O_2) and F(300W, 10sccm O_2).

The SEM micrographs (topographical view) of the silver and silver oxide films deposited under different deposition power and oxygen flowrates shown in Figure 3 indicate a mixed morphology composed of compact nanostructure and lamellae with aggregate particulate structure having porous and compact surfaces [15-17].

Images A, B, C, and D in the Figure 3 for the films obtained with the same oxygen flow rates but different power show a correlation between the power and layer structure. It can be seen that the film deposited at higher deposition powers possess denser columnar structures compared to the films prepared at lower deposition powers.

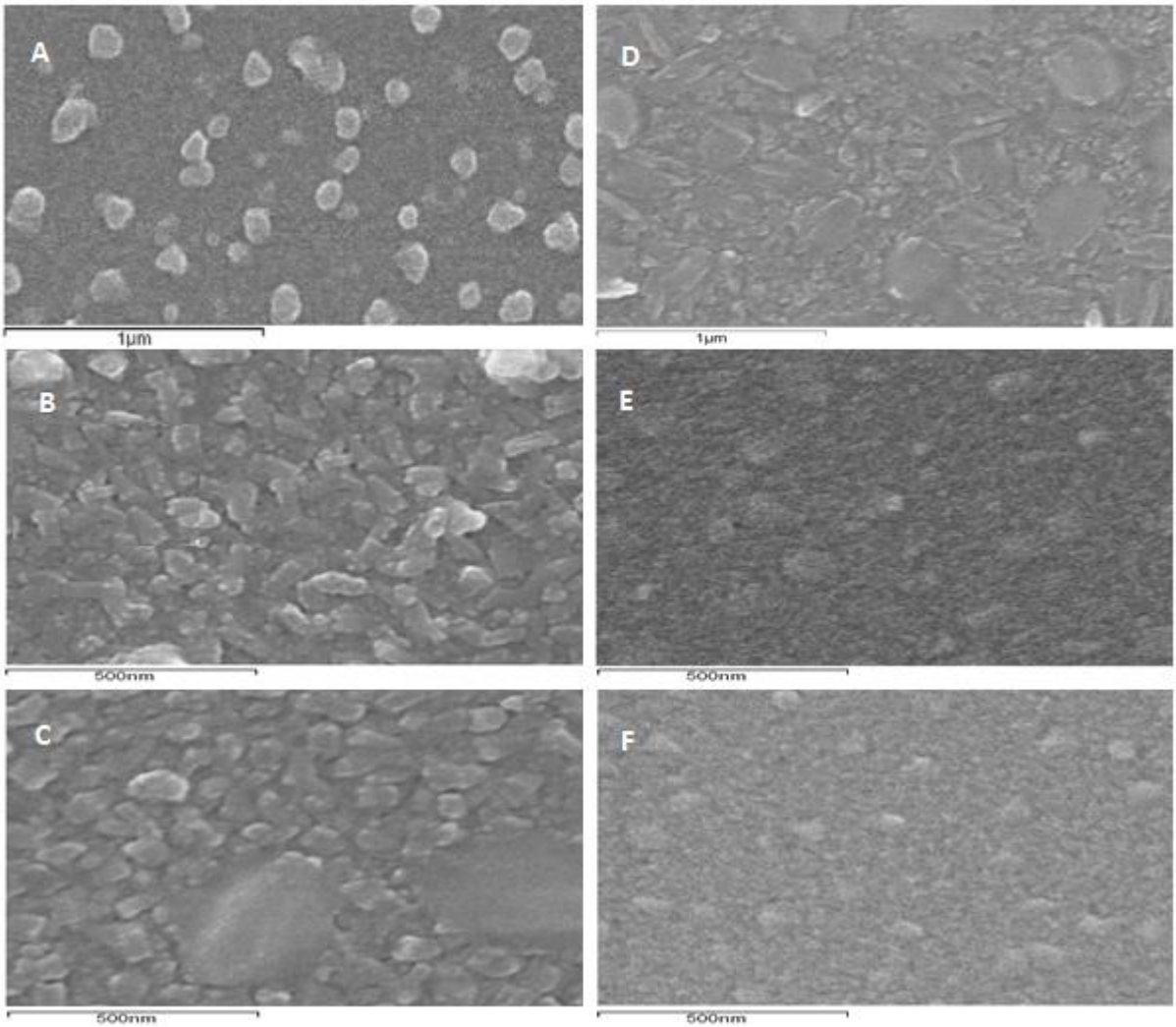

Figure 3: SEM micrographs of the surface of thin films at different power and O_2 flow rates with deposition time of 2 minutes. A(100W, 4sccm O_2), B(200W 4sccm O_2), C(250W, 4sccm O_2), D(300W, 4sccm O_2), E (300W, 8sccm O_2) and F(300W, 10sccm O_2)

The energy dispersive X-ray (EDX) analysis was also used as an attachment to the electron microscope (SEM) analysis to analyze the chemical components of the films. The method detects the X- ray produced as a result of the interaction of the electron beam with the sample. Figure 4 shows typical EDX spectra of thin films deposited under different conditions. Figure 4-A shows EDX spectrum of the film deposited in the absence of oxygen in the chamber indicating the presence of different phase of Ag in the film. Figures 4-B and 4-C show the EDX spectra of films deposited in presence of oxygen. The oxygen and Ag peaks confirm the formation of silver oxide films on the substrate. The Si peak appeared on the EXD spectrum in figure 4-B is due to the presence of chemical element silicon in the glass substrate which is masked with increase in the film thickness as the deposition power is increased. These results are confirmed by XRD analysis of the films as follow.

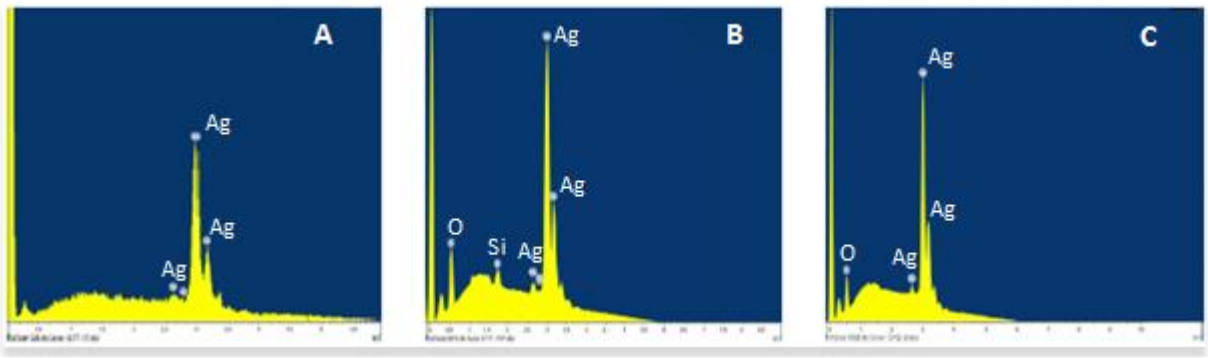

Figure 4: EDX spectra of films deposited at: A) 300W, 0sccm O_2. B) 200W, 6sccm O_2. C) 400W, 4sccm O_2.

3.2. XRD results

XRD analysis of the thin films were carried out to investigate power and O_2 flow rates dependency of the chemical composition and oxidation state of silver oxide thin films deposited on the substrate. The XRD study of the crystalline structure of the deposited films shows that the crystalline structure and oxidation state of silver oxide thin films formed on the surface strongly depend on the power and oxygen flow rate used during the deposition process. The XRD spectra of the films deposited in the absence of oxygen in the chamber shown in Figure 5 indicate the deposition of pure silver films with FCC structures corresponding to the intense (111) and (200) peaks of crystal planes of Ag at 38.1° and 44.3° respectively [18-22]. Sharp and well defined peaks are observed in the silver XRD spectra for all deposition forward powers. The appearance of low intensity peaks at 64.4°, 77.4°, 81.5° and 98.7° on XRD spectra indicates the presence of different phases of pure silver with Miller indices (220), (311), (222) and (400) in the silver target respectively [18, 20-23].

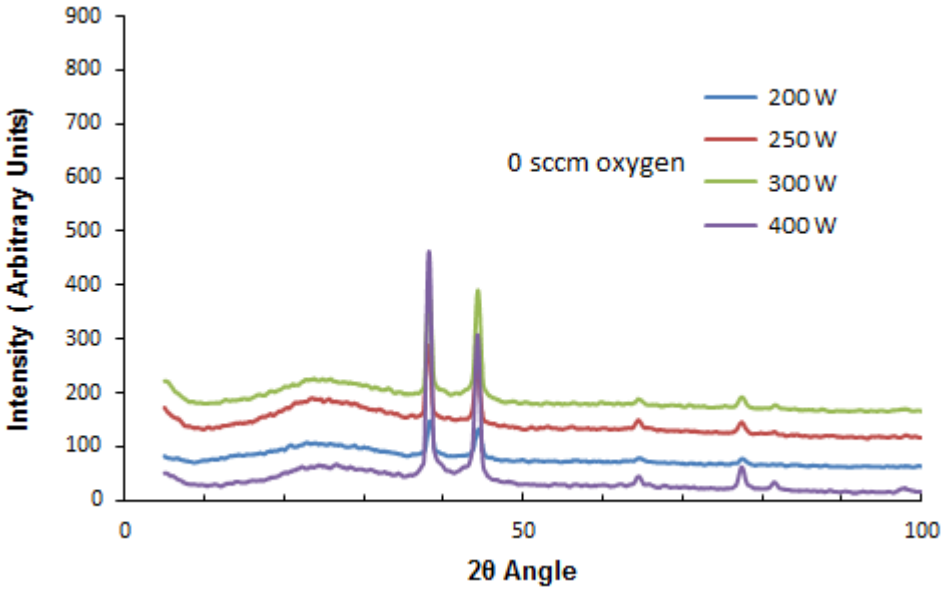

Figure 5 XRD patterns for Ag films deposited at different deposition powers in the absence of oxygen.

The XRD spectra of films deposited when oxygen was introduced to the chamber in Figure 6 show the development of a bi-phase system indicating that the films are comprised of both silver and silver oxide at its different oxidation states.

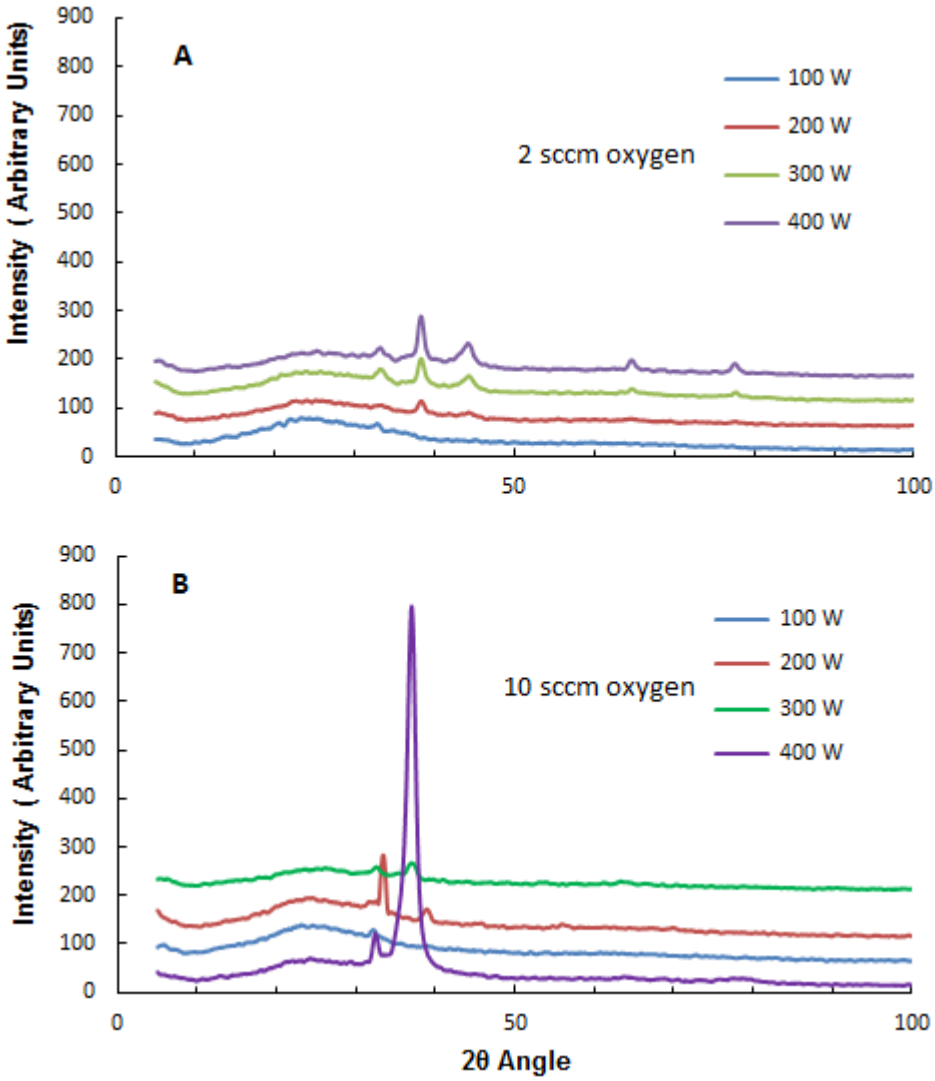

Figure 6: XRD spectra of films deposited at different deposition powers under A) 2sccm O_2, B) 10sccm O_2.

Analysis of the XRD patterns shown in Figures 6-A and 6-B indicates that increasing oxygen flow rate results in a progressive increase in the Ag_2O diffraction peaks with a Miller indices of (111) and (101). When the oxygen flow rate is increased in the chamber, the sputtered metal atoms of silver react with the oxygen atoms to form oxides of silver in the presence of the plasma. From the X-ray diffraction measurements given in Figures 6-A and 6-B one can observe that the intensity corresponding to the metallic silver diminishes while the intensity of oxides of silver increases with increase in the oxygen flow rate. It has been discussed that different phases of silver oxides (AgO, Ag_4O_4, Ag_2O) can be formed at different oxygen flow rates with different crystalline orientations and angles [18, 24].

The XRD spectra of silver oxides deposited at 100 W under 2 and 10 sccm oxygen show only a weak peak at 33.14° with Miller index of (-102) corresponding to the monoclinic phase of AgO. The spectra generally improved in shape and quality with increase in sputtering forward power. There is corresponding increase in the intensity of the Ag_2O (111) and Ag_2O (200) peaks with increase in the deposition power. The peaks become sharper, with the sharpest and best defined peaks obtained at a deposition power of 400W. The XRD spectra of the films obtained under different deposition conditions indicate that a set of thin film electrodes with thickness of 50 to 150 nm comprised of silver/silver oxide with different oxidation states can be prepared by magnetron sputtering when controlling the sputtering power and oxygen in the chamber.

TABLE 1: XRD results of the sputtered films showing the presence of different phases of silver oxide and their angle obtained at different oxygen flow rates and deposition powers.

Sputtering Conditions		Angle of incidence diffraction (XRD)	Phases of silver oxide
O_2 flow rate	Power (W)		
2 sccm	100	33.2	AgO(-102)
	200 W	38.2	Ag_2O(101)
		44.1	Ag_2O(200)
	300 W	33.2	AgO(-102)
		38.2	Ag_2O(101)
		44.1	Ag_2O(200)
		64.5	Ag(110)
		77.7	AgO(311)
	400 W	33.2	AgO(-102)
		38.2	Ag_2O(101)
		44.1	Ag_2O(200)
		64.5	Ag(110)
		77.7	AgO(311)
10 sccm	100 W	32.0	AgO(200)
	200 W	33.2	AgO(-102)
		38.2	Ag_2O(101)
	300 W	32.5	Ag_2O(111)
		36.9	Ag_2O(002)
	400 W	32.5	Ag_2O(111)
		36.9	Ag_2O(002)

Table 1 summarizes XRD results of the sputtered films showing different phases of silver oxide and their angle obtained at different oxygen flow rates and deposition powers. It can be seen that Ag_2O becomes the dominant phase and the other phases of silver oxide diminish with increase in the deposition power and oxygen flowrate. This observation was expected since Ag_2O is the most thermodynamically stable oxide of silver compared to the other oxide phases of silver [25]. The Ag_2O phase possesses a simple cubic structure with a lattice parameter of 0.4728nm at room temperature [26]. The intensity of the Ag_2O peaks also increases at higher oxygen flow rates and higher deposition powers as shown in Figures 6A and 6B [24].

3.3. Contact Angle and Surface Energy Measurements

A better understanding of the wettability of the silver oxide thin films by different types of electrolytes is crucial for their superior capacitance, rate capability and energy storage performance when used as electrode for storing energy in supercapacitors. Contact angle measurement is a widely accepted method for characterizing surfaces. Contact angle and surface energy measurements provide information on the wettability of surfaces, whether a liquid droplet sticks or is removed from a surface or it spreads or remains at the point of contact. In small contact angles (below 90 degrees) the liquid spreads on the surface well indicating a high solid surface energy or chemical affinity, and consequently a relatively high degree of wetting. Large contact angles (above 90 degrees) indicate poor wettability [27, 28] with a low solid surface energy or chemical affinity. If the water contact angle is smaller than 90°, the solid surface is considered hydrophilic and in case of the water contact angle larger than 90° the solid surface is considered hydrophobic.

Since the measured contact angles depends on the nature and the properties of the probe liquid in contact with the surface in addition to the properties of the surface itself [29], three different liquids with different polar-dispersive characteristics are used to reflect the effect of liquid nature and surface characteristics of the films on their wettability with the probe liquids. Water is used as the polar liquid; diiodomethane used as the most dispersive liquid and ethylene glycol is used as a liquid with a median polar-dispersive nature. The wettability of silver/solver oxide thin films in contact with water, ethylene glycol and diiodomethane were investigated by measuring the contact angles using a computer controlled KSV Ltd CAM 200 goniometer system. The choice of these liquids with a wide range of polar-dispersive nature will help in understanding the wetting response of the thin films surfaces when in contact with different electrolytes. The variation of contact angle of the liquid on the films prepared at different oxygen flow rates at various forward powers during deposition for three probe liquids are presented in Table 2. All films deposited under different

conditions exhibited the highest contact angles with water as the most polar liquid, and the lowest contact angles were obtained with diiodomethane as the most dispersive liquid and the median contact angles were obtained with ethylene glycol with median polar-dispersive nature. The contact angles of the silver oxide films when in contact with water showed little variation with the deposition power. However, the variation of contact angle with oxygen flow rate at various forward powers during the deposition of the films are less than 90 degree showing the silver oxide films are relatively hydrophilic. There is a progressive decrease in contact angle with increasing the oxygen flow rate.

TABLE 2: Contact angles of different liquids with silver oxide films deposited at different oxygen flow rates and deposition powers.

Sputtering Conditions		Contact Angles		
Power (W)	O_2 flow rate (sccm)	Water (polar)	Diiodomethane (dispersive)	Ethylene Glycol (median nature)
200 W	2	87.9	44.3	75.5
	4	76.8	43.7	67.2
	6	69.2	33.4	63.5
250 W	2	87.3	43.1	71.4
	4	79.1	48.3	72.3
	6	72.2	42.9	70.6
	8	62.0	36.9	60.7
300 W	2	89.5	59.3	86.4
	4	81.7	41.0	76.5
	8	79.0	38.2	60.5
	10	77.3	34.4	63.6
400 W	2	83.2	38.6	71.1
	6	80.1	48.9	71.6
	8	78.0	35.4	68.5
	10	77.3	34.4	63.6

Good surface wettability by a liquid requires both appropriate surface roughness and surface energy. For a liquid to effectively wet a surface the surface energy of the wetting liquid must be as low as or lower than the surface energy of the substrate to be bonded or, the surface energy of the substrate must be raised. The wettability of a surface is determined by the outermost chemical groups of the solid. Differences in wettability between surfaces that are similar in structure are

mainly due to differences in packing of the atoms. In the case of silver oxide thin films change in the oxidation state of the films, changes their affinity toward the probe liquids. It can be noticed that increasing oxygen flow rate increases the wettability of the films toward water further, as a result of change in the electronic properties of the surface due to the increase in the oxidation state of the films. This is because of clustering of electrons in polar molecules of water around the oxides at a higher oxidation state. The results show that the effect of electronic structure of the films' surfaces on their wettability with the probing liquid is more dominant than the effect of their surface morphology. As discussed by SEM micrographs before, higher oxygen flow rates result in smooth and dense films expected to decrease their wettability with water, however due to their improved electronic properties, films obtained at higher oxygen flow rates show better wettability toward water.

Different characteristics of the film surfaces will affect their physical and chemical interactions with the liquid electrolyte that will probably be reflected in their bonding strengths. The surface property most frequently correlated with this adhesion is surface-free energy, a measure of the capacity of a surface to interact spontaneously with other materials by forming new bonds, often expressed as the related parameter, surface tension (γ), which is a measure of surface wettability [30, 31]. The surface energy is defined as the adhesion work necessary to separate solid – liquid surfaces beyond the range of the forces holding them together given as energy per unit area. It is quantitatively determined from the interactions between the surface of thin films deposited under different sputtering conditions and a series of probe liquids of different interfacial properties.

Table 3 shows various components of surface energy of the silver oxide films evaluated using the Fowkes, Wu and Acid/ Base methods. The total surface energy (γ^{tot}) of deposited films and the probe liquids depends on the interfacial intermolecular forces and is considered to be the sum of dispersive interactions (van der Waals) and polar interactions.

The quantitative determination of the various components of surface energy would allow selection of appropriate film/liquid pairs with a superior wetting behavior. As shown in Table 3 in all the surface energy measurements taken, the predominant term is the dispersive term (γ^{d}) and the values of the polar component (γ^{p}) of the surface energies of the silver oxide thin films are small compared to the dispersive components of the surface energy.

TABLE 3: The Fowkes, Wu and Acid-Base (AB) surface energy terms of silver oxide thin films prepared at various ranges of deposition powers and oxygen flow rates.

Sputtering Conditions		Surface Energy (mJ/m^2)								
Power (W)	O_2 flow rate (sccm)	Fowkes			Wu			Acid-Base (A/B)		
		γ^d	γ^p	γ^{Tot}	γ^d	γ^p	γ^{Tot}	γ^{LW}	γ^{AB}	γ^{Tot}
200 W	2	31.54	1.56	33.10	35.90	2.60	38.50	37.38	-5.63	31.75
	4	31.16	4.87	36.03	34.76	6.87	41.63	37.67	-5.98	31.69
	6	34.11	6.62	40.73	37.89	8.84	46.73	42.75	-9.86	32.89
	10	41.40	1.54	42.94	47.01	2.86	49.87	50.80	-11.07	39.73
250 W	2	33.01	1.60	34.61	36.60	3.05	39.65	38.02	-3.89	34.13
	4	28.29	4.93	33.22	32.54	6.44	38.98	35.20	-7.73	27.47
	6	29.59	6.51	36.10	34.01	8.04	42.06	38.16	-11.39	26.77
	8	31.93	10.46	42.39	35.53	12.54	48.07	41.19	-10.84	30.35
300 W	2	22.73	2.48	25.21	28.48	2.75	31.23	28.96	-8.53	20.43
	4	31.09	2.84	33.92	36.27	3.86	40.13	39.10	-10.45	28.65
	8	35.62	3.52	39.14	38.09	6.17	44.26	40.49	-2.49	38.00
	10	35.80	3.70	39.51	39.09	6.04	45.13	42.31	-5.49	36.82
400 W	2	33.81	2.26	36.07	37.90	3.79	41.69	40.29	-6.34	33.95
	6	28.71	4.28	32.99	32.70	5.91	38.61	34.89	-6.04	28.86
	8	34.34	3.52	37.86	38.44	5.36	43.80	41.83	-8.06	33.77
	10	37.11	4.25	41.36	40.18	6.86	47.o4	43.81	-5.42	38.39

Figure 7 shows the contribution of these different interactions to the total surface energy of the films obtained by Fowkes method. It can be noticed that the dispersive components of the surface energy become even more predominant when the silver oxide thin films are deposited at higher oxygen flow rates. This explains the good interaction/wettability of the water on the films deposited at higher oxygen flow rates. The results are in good agreement with the resulting low contact angles for the films deposited at higher O_2 flow rates showing that the stoichiometry of the surface determined by the interaction of oxygen and silver is a determining factor in the surface energy of the films.

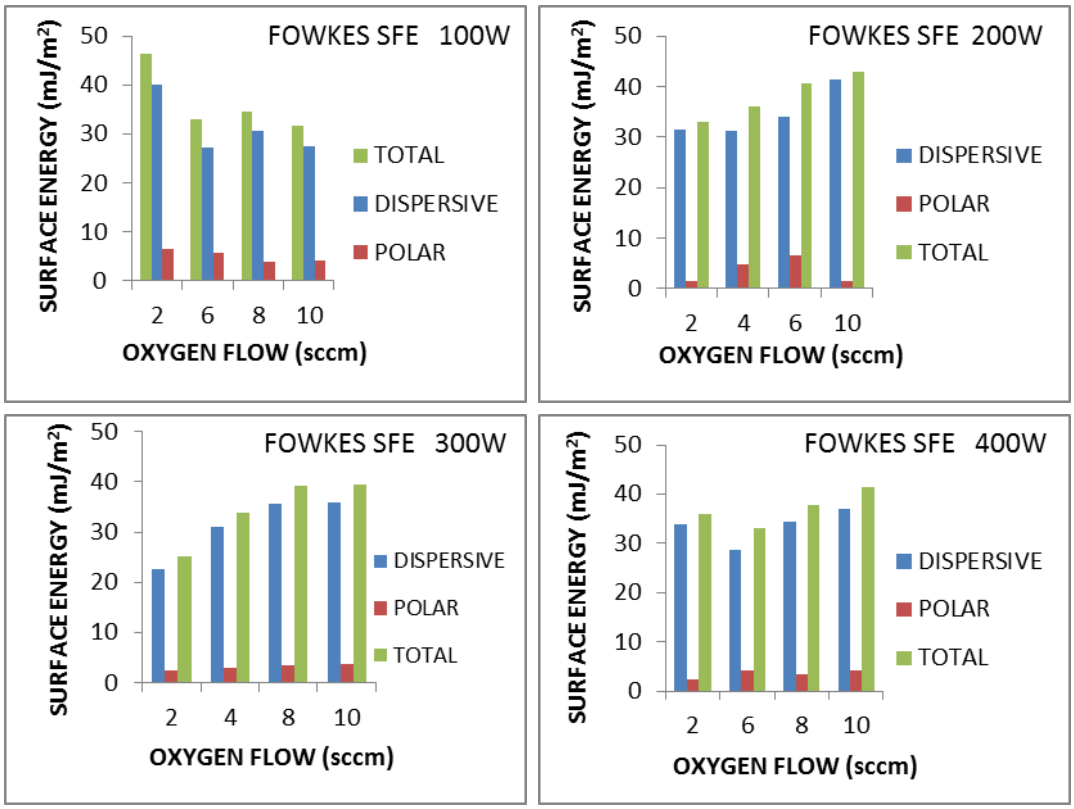

Figure 7: Various components of surface free energy (SFE) of the silver oxide thin film deposited at different forward powers and oxygen flow rates.

4. CONCLUSIONS

Silver oxide thin films have been deposited by magnetron sputtering technique using argon and oxygen as the sputtering and reactive gas respectively. The films were characterised by SEM, EDX, XRD and contact angle measurements (goniometry) to investigate the effects of the sputtering conditions on their morphology, stability, growth rate, and wettability with different probing liquids as promising electrode materials for supercapacitor applications. The SEM micrographs of the films showed that the average thickness of the films can be controlled in the range of 50 – 330 nm by controlling the deposition conditions. The thickness of the silver oxide films increased with increase in the deposition power. There is a decrease in the thickness of the films with increase in O_2 flow rate. It is shown that films with smooth surface and compact structure can be obtained at higher deposition powers and higher O_2 flow rates.

The XRD results showed that the oxidation state of thin films can be controlled when varying the oxygen flow rate. Ag_2O oxide phase becomes the dominant phase at higher oxygen flow rates and higher deposition powers. The results obtained through contact angle and surface energy measurements also revealed that films with better wettability toward water can be produced at higher oxygen flow rates.

ACKNOWLEDGMENT

We are grateful to COST action MP1106 for supporting this work and providing opportunities for fruitful discussions during its meetings.

REFERENCES

[1] P. J. Hall, M. Mirzaeian, S. I. Fletcher, F. B. Sillars, A. J. R. Rennie, G. O. Shitta-Bey, G. Wilson, A. Cruden and R. Carter, *Energy Environ. Sci.*, 2010, 3, 1238–1251.

[2] W. Dmowski, T. Egami, K. E. Swider-Lyons, C. T. Love and D. R. Rolison, *J. Phys. Chem. B*, 2002, 106, 12677–12683.

[3] T. D. Dang, T. T. H. Le, T. B. T. Hoang and T. T. *Mai, Adv. Nat. Sci.: Nanosci. Nanotechnol*., 2015, 6, 025011.

[4] F. I. Dar, K. R. Moonoosawmy , M . Es-Souni, *Nanoscale Res Lett.*, 2013, 23, 363

[5] J. Xu, L. Gao, J. Cao, W. Wang, Z. Chen, *Electrochimica Acta*, 2010, 56, 732–736

[6] Y. Wei, J. Zhu, and G. Wang, *IEEE Transactions on Applied Superconductivity*, 2014, 24 (5).

[7] P. Lorkita, M. Panapoya, B. Ksapabutr, *Energy Procedia*, 2014, 56, 466 – 473.

[8] E. Chibowski and K. Terpilowski, in K. L. Mittal (ed), "Contact angle, wettability and adhesion", vol. 6, Brill/VSP, Leiden, Boston, 2009, 284-299.

[9] R. P. Schneider, *J. Adhesion Sci. Technol.* 1997, 11, 65-93.

[10] R. P. Schneider, B. R. Chadwick, R. Pembrey, J. Jankowski and I. Acworth, *FEMS Microbiol. Ecol.* 1994, 14, 243-254.

[11] J. Kloubek, *Adv. Colloid Surfaces Sci.*, 1992, 38, 99-142.

[12] D. K. Owens and R. C. Wendt, *J. Appl. Polym. Sci.*, 1969, 13, 1741-1747.

[13] A. A Ogwu, E. Bouquerel, O. Ademosu, S. Moh, E. Crossan, and F. Placido, *Metallurgical and Materials Transactions A*, 2005, 36A, 2435-2439.

[14] R. J Good, *J. Adhesion Sci. Technol.*, 1992, 6, 1269-1302.

[15] H. Tang, K. Prasad, R. Sanjines, P.E. Schmid and F. Levi., *J. Appl. Phys.*, 1994, 75, 2042.

[16] T.S Moss. *Optical properties of Semiconductors, Butterworth*, London, 1959

[17] L.J. Meng, and M.P. Dos Santos, *Thin Solid Films*, 1993, 226, 22-29.

[18] U. K Brik, S. Srinivasan, C. L. Nagendra, A. Subramanyam, *Thin Solid Films*, 2013, 429, 129-134.

[19] H. J. Jeon, S. C. Yi, S. G. Oh, *Biomaterials*, 2003, 24, 4921-4928.

[20] F. Meng, Z. Sun, *Applied Surface Science*, 2009, 255, 6715-6720.

[21] J. P. Ruparelia, A. K. Chatterjee, S. P. Duttagupta, S. Mukherji, *Acta Biomaterials*, 2008, 4, 707-716.

[22] X. Y. Gao, H. L. Feng, J. M. Ma, Z. Y. Zhang, J. X. Lu, Y. S. Chen, S. E. Yang, J. H. Gu, *Physica B Condensed Matter*, 2010, 405, 1922-1926.

[23] X. Y. Gao, S. Y. Wang, J. Li, Y. X. Zheng, R. J. Zhang, P. Zhou, Y. M. Yang, L. Y. Chen, *Thin Solid Films*, 2004, 455-456, 438-442.

[24] P. N. Reddy, M. H. Prasad Reddy, J. F. Pierson, and S. Uthann, *ISRN Optics*, 2014, Article ID 684317, http://dx.doi.org/10.1155/2014/684317

[25] W.-X. Li, C. Stampfl, & M. Scheffler, *Physical Review B.*, 2003, *68*(16), 165412-1-165412-15

[26] S. Ma, J. Xue, Y. Zhou and Z. Zhang, *J. Mater. Chem. A*, 2014, 2, 7272

[27] R. P. Schneider and K. C. Marshall, *Colloids Surfaces B: Biointerfaces*, 1994, 2, 387-396.

[28] R. J. J. Good, *Adhesion Sci. Technol.*, 1992, 6, 1269-1302.

[29] A. A. Ogwu *et al*., *Acta Materialia*, 2005, 53, 5151–5159

[30] Baier, R. E., *In Proc. Third International Congress Marine Corrosion and Fouling*, 1973, pp. 633–639.

[31] Becka, A. & Loeb, G., *Biotech. Bioen.*, 1984, 26, 1245–1251.